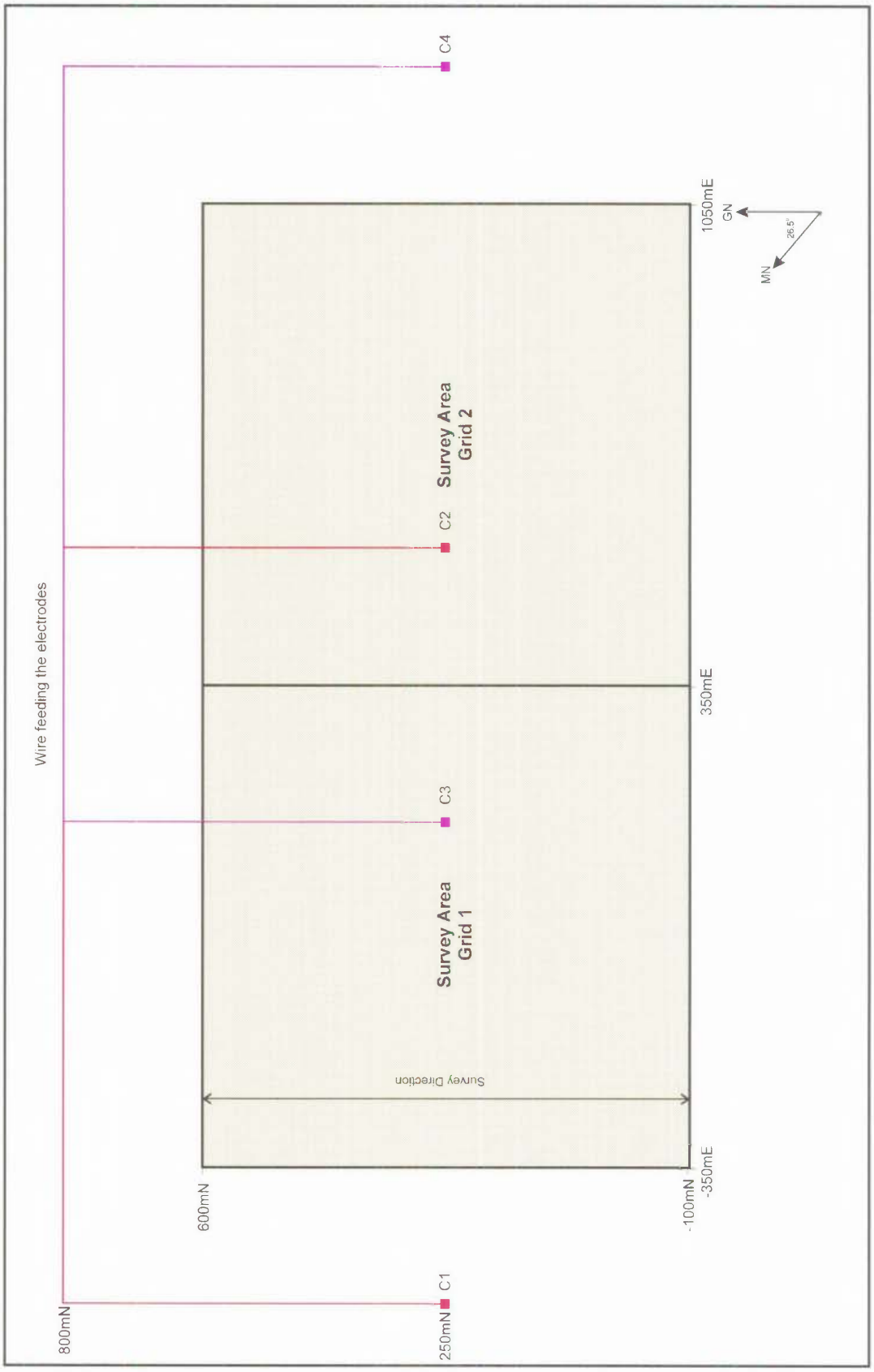

Figure 6-8. Layout of the Survey Area showing the locations of electrodes C1, C2, C3 and C4 and current-bearing wire.

6.2.5 Results

6.2.5.1 Total Magnetic Intensity

The magnetics component of the SAM data are presented in Figure 6-9 as upward continued (2 m) Total Magnetic Intensity and in Figure 6-10 as reduced to the pole (RTP). In both images, the geology from Figure 6-3 has been overlayed. The colour assignment ranges from purple for low amplitudes to red for high amplitudes. Slanted light illumination has been applied to the images from an azimuth of 200° local (inclination: 30°). Upward continuation was applied to the data due to the high degree of near surface magnetic contamination from both cultural and geological sources.

Foley *et al.* (1995) describe several clearly recognisable responses in the magnetics:

- a large ovicular response centred on 100 mE, 150 mN (Orlando West) due to a magnetic source modelled at 220 m below the surface with several apophyses extending nearer to the surface.
- a smaller, more complex feature to the east of the above, centred on 450 mE, 175 mN, coincident with the previous underground resource.
- the relatively non-magnetic response of the Tennant Creek Granite, and
- an underlying deeper seated (longer wavelength) response associated with the Warramunga Sediments - Tennant Creek Granite contact, which dips to the south (local).

The Orlando magnetic anomalies are due to ironstone bodies. However, there is no discrete magnetic response associated with the currently mined resource which is essentially hosted by chloritic sediments +/- quartz-magnetite stringers parallel to a thin ironstone unit.

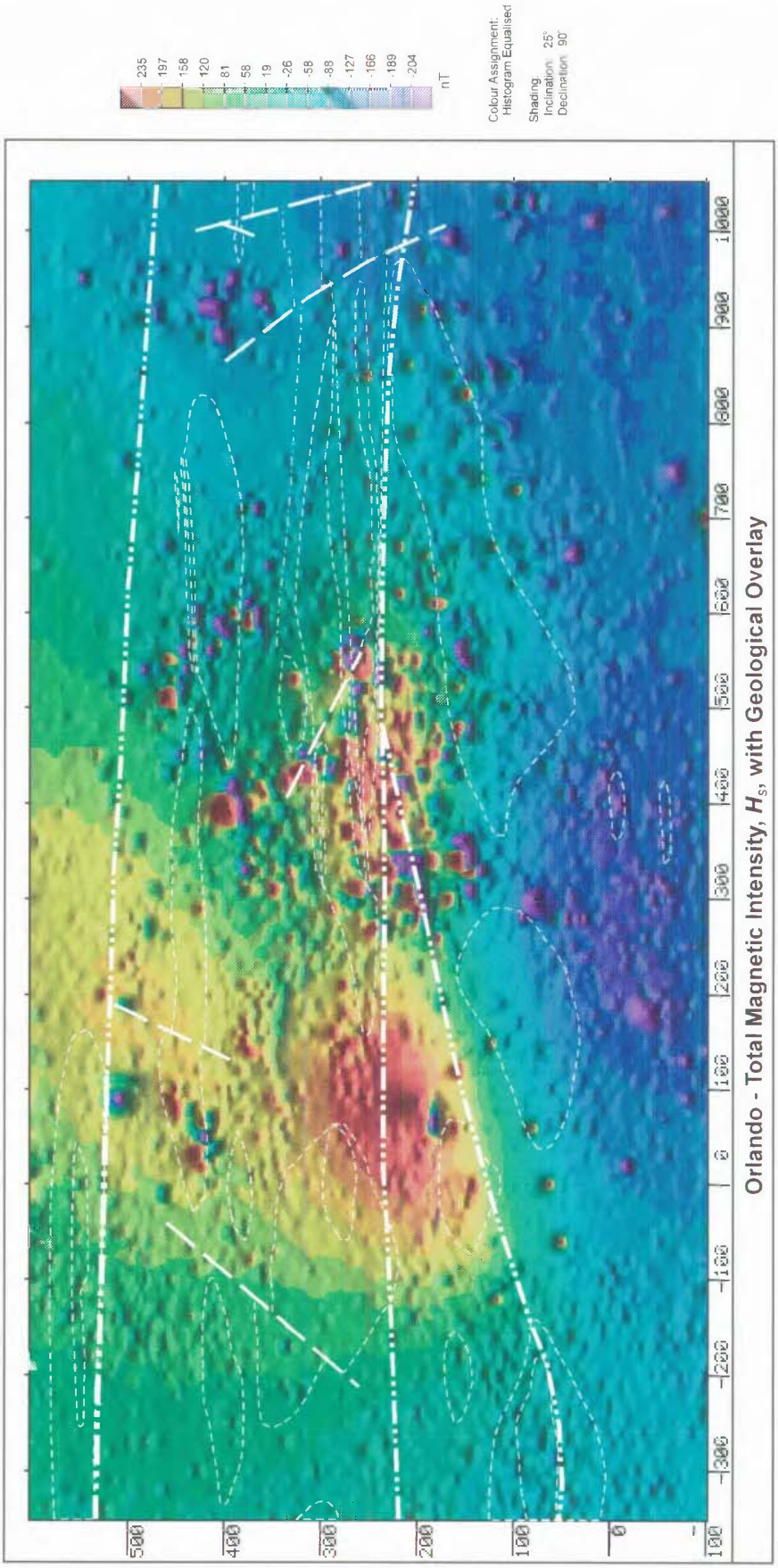

Figure 6-9. Orlando - Total Magnetic Intensity, H_S, with geological overlay.

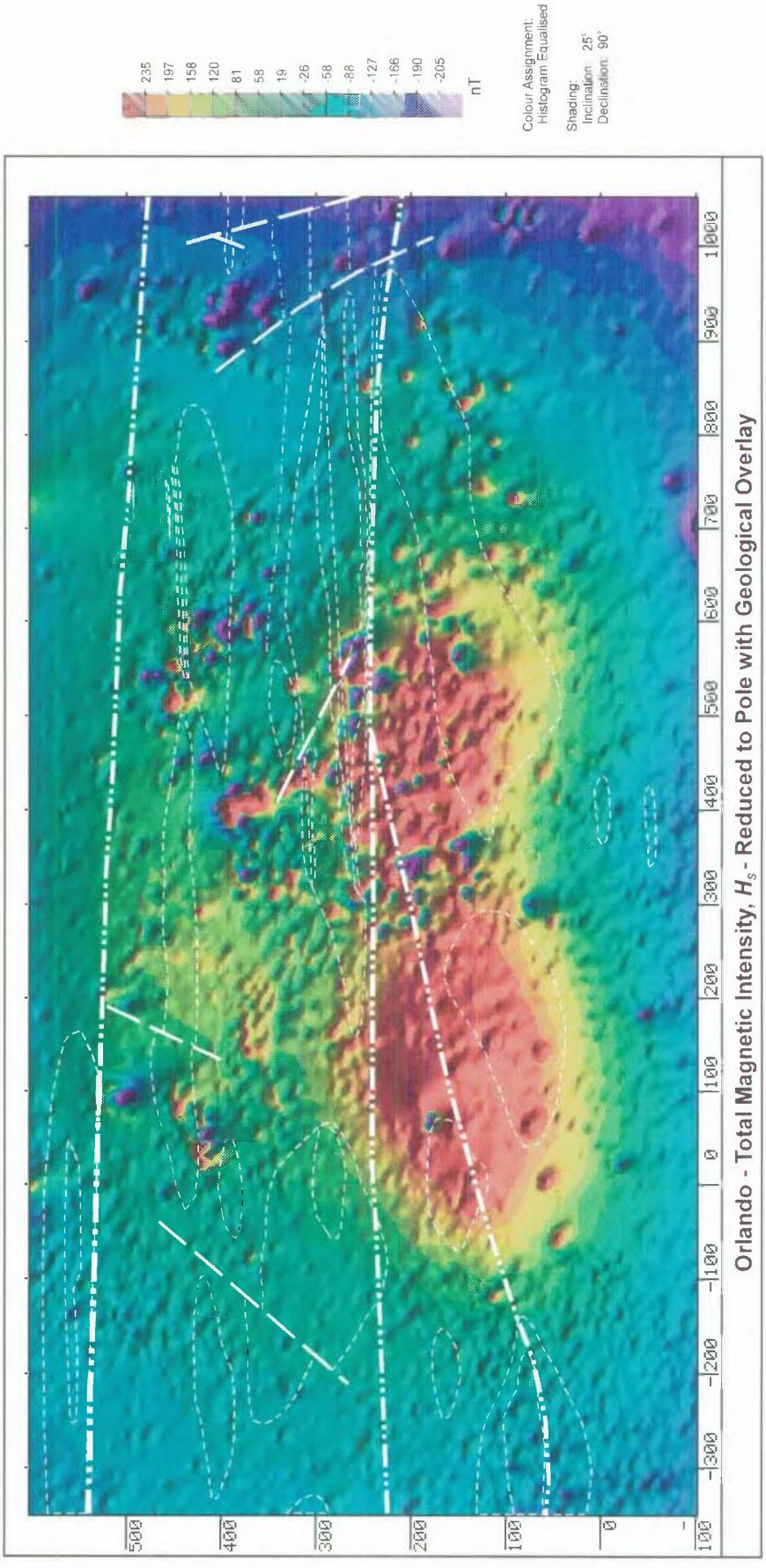

Figure 6-10. Orlando - Total Magnetic Intensity, H_S - Reduced to the Pole.

6.2.5.2 Total Field Magnetometric Resistivity (TFMMR)

The transmitted signal reverses in direction continuously during the survey and for each direction of current flow, the TFMMR data exhibit a dominant polarity, although data of both polarities was found to be common. Consequently, a polarity convention must be chosen for presentation purposes. The most practical convention is that the predominant polarity in the recorded data is made positive. That is, high amplitude signals will appear positive. In this case, the convention selected was for current flowing west to east.

The TFMMR data were processed separately but normalised for current flow. Images of normalised TFMMR for both Grids 1 and 2 are shown in Figure 6-11. No attempt was made to append the two images together. Again, the colour assignment is such that purple colours represent low amplitude data and high amplitudes are represented by red. Slanted light illumination was again applied from an azimuth of 200° and the geology from Figure 6-3 was overlayed.

The difficulty in detecting polarity reversals in the TFMMR data were described earlier. In the case of the Orlando data, the point of polarity reversal occurred in a low gradient area which made picking the actual point of reversal quite difficult. This was largely due to the fact that the polarity of the data appeared to oscillate about the zero level. The resulting error in determining the point of reversal resulted in an obvious linear artefact in the images which is shown on Figure 6-11 as a red dashed line. As can be seen from the figure, the point of reversal continued through the two grids, although some mismatch occurred at the boundary of the two grids. The blue dashed line indicates the location of a live mains power line.

The two images are generally quite similar with low amplitude signal over the resistive units to the north of the Orlanco shear and high amplitude data over the more conductive unit to the south of the shear. The Orlando shear itself coincides with a sharp transition between the low and high signal amplitudes.

The secondary shear is also clearly evidenced in the westernmost grid (Grid 1) by a more subtle but distinct linear anomaly, again with a relative low to the north and a high to the south.

Within the low to the north of the shear are a series of apparently continuous sub-parallel anomalies which are believed to arise from resistivity contrasts within a series of units comprising silicified siltstones, metasiltstones and hematitic siltstones. Of particular interest is a linear anomaly extending from 550 mE to 900 mE at about 250 mN. The anomaly terminates abruptly on both ends suggesting that the source may be fault-bound. The anomaly also coincides with the location of the current open cut mining operation.

To the south of this anomaly are a number of major, very distinct linear anomalies which would appear to reflect major geological structure. Unfortunately, little is known about the geology in this area and it is not known what the sources of the anomalies are. Other features of the dataset include very fine linears some of which appear to coincide with known faults.

An obvious feature of the data sets is the fact that the two images do not match very well, particularly south of the shear. To some extent, this is to be expected due to the dependence of current channelling on the location of the electrodes. However, the main reason for the mismatch is believed to be due to the fact that the TFMMR anomaly is a total field anomaly and, as has been described earlier, is influenced by the attitude of the Earth's magnetic field. An attempt to correct the data was made by applying standard reduction to the pole techniques in order to correct the asymmetry. The result of the procedure is shown in Figure 6-12.

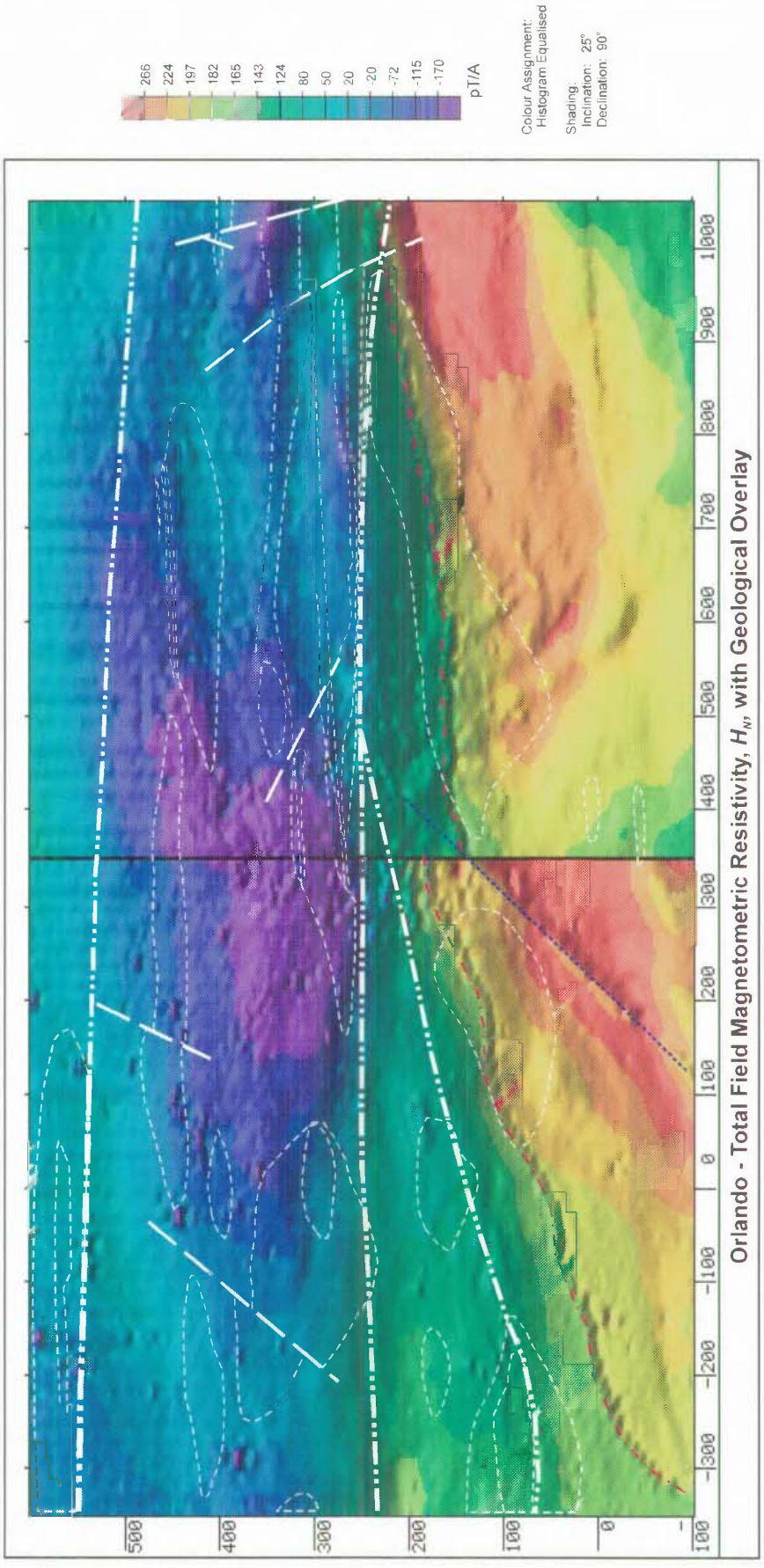

Figure 6-11. Orlando - Normalised TFMMR, H_N with geological overlay.

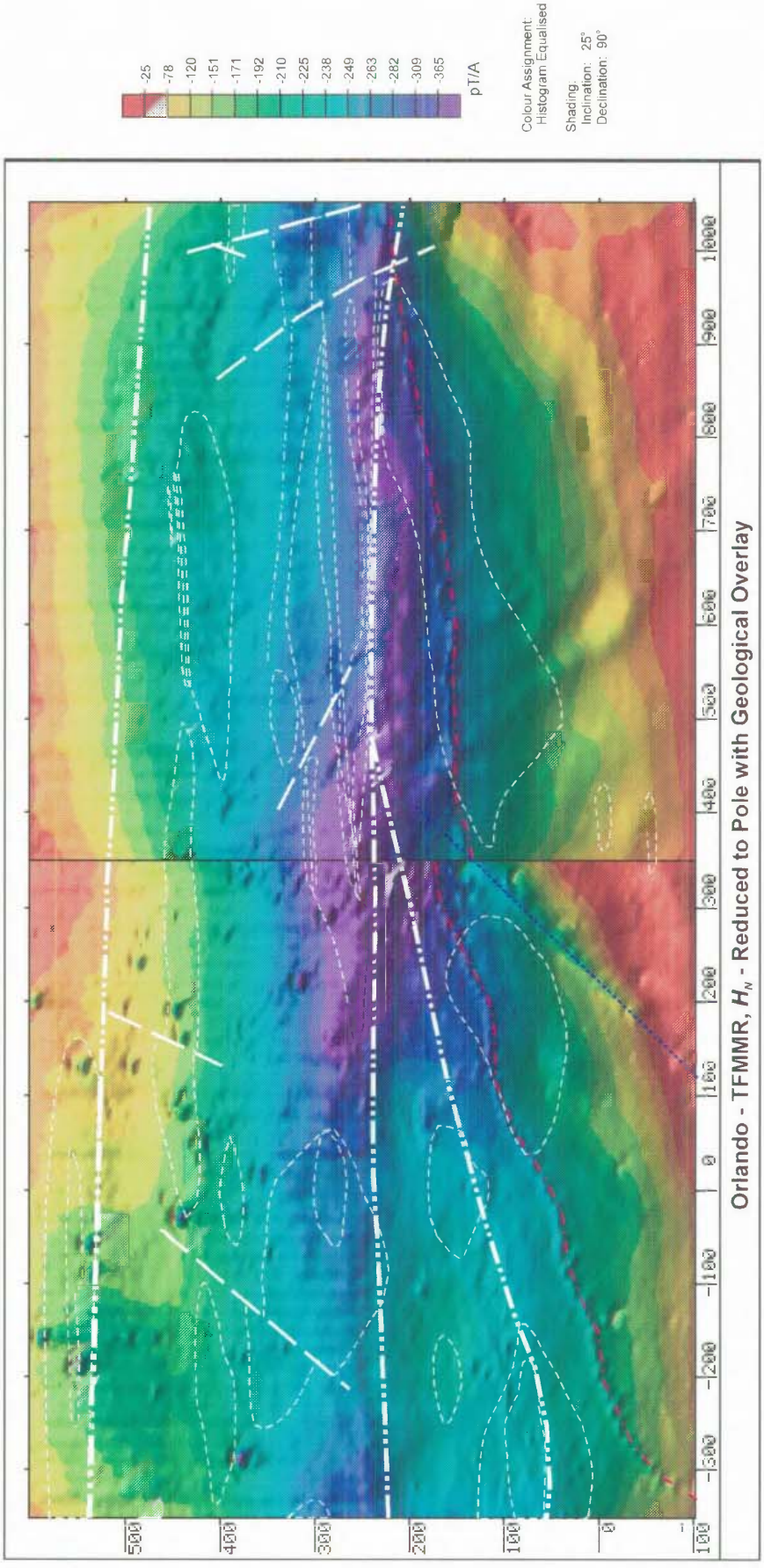

Figure 6-12. Normalised TFMMR, H_N - Reduced to Pole.

6.3 Feasibility Study #2 - Flying Doctor Deposit, Broken Hill, New South Wales

6.3.1 Location

The Flying Doctor Deposit, named due to its proximity to the Royal Flying Doctor Radio Control Centre, is located approximately 5 km northeast of Broken Hill. The area lies along strike from the main ore bodies and is considered highly prospective for the development of sulphide mineralisation. A locality and regional geology map of the area is shown in Figure 6-13.

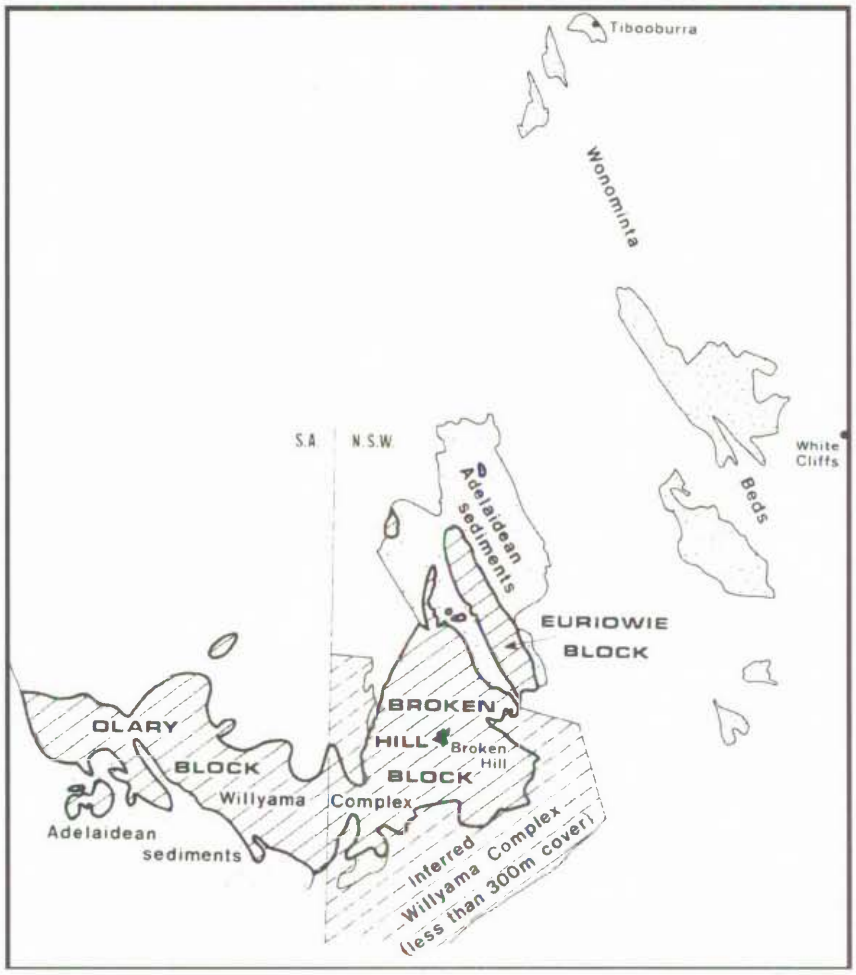

Figure 6-13. Locality and Regional Setting for Broken Hill (After Stevens *et al.*, 1980).

The deposit was originally detected by Induced Polarisation profiling techniques as a zone of intense anomalies. Subsequent drilling in 1965 led to the discovery of a

massive sulphide body. The most recent drilling in 1980 delineated what has until recently been described as sub-economic mineralisation with reserves of 300,000 tonnes averaging 5.7% Pb, 59 g/t Ag and 3.0% Zn (Widdop *et al.*, 1983). Over the last 20 years, comprehensive geological and geophysical data have been acquired at the site and, consequently, the Flying Doctor Deposit has become an important test site for the evaluation of new geophysical techniques in the Broken Hill region.

6.3.2 Geological Setting

The geology of the Flying Doctor prospect has been comprehensively described in reports by Stevens *et al.* (1980) and Widdop *et al.* (1983). The majority of the known stratiform and strata-bound base-metal mineralisation in the Broken Hill Block occurs in two metamorphic rock suites. These are the Thackaringa Group and the overlying Broken Hill Group both of which are part of the Willyama Supergroup (Stevens *et al.*, 1980). Widdop *et al.* (1983, 5) state that

> *"The known Broken Hill type Pb-Ag-Zn mineralisation occurs within the Broken Hill group which consists of a variable sequence of metasedimentary gneisses, quartzo-feldspathic gneisses, pegmatites, amphibolites, iron formations and the so-called 'lode-horizon' rocks".*

At the Flying Doctor prospect, two separate lode horizons have been delineated: the upper lode horizon (ULH) and the main lode horizon (MLH). The MLH is the direct extension of the lode horizon containing the main Broken Hill orebodies. The ULH is most likely a structural repetition of the MLH. There is an intimate association between the lode horizon rocks (commonly quartz gahnite, garnet quartzite and garnet sandstone) and the development of Pb-Ag-Zn sulphide mineralisation and they are generally interpreted as metamorphosed, locally remobilised, chemical sediments, deposited together with the stratiform sulphides.

A geological map of the Flying Doctor prospect is included as Figure 6-14. Much of the early exploration work conducted in the area was based on the imperial grid system shown. Three principal survey lines with a separation of 750′ (228.6 m) were established at the site and are shown as Lines 24.50, 25.25 and 26.00. Geological cross sections along these lines are shown in Figure 6-15.

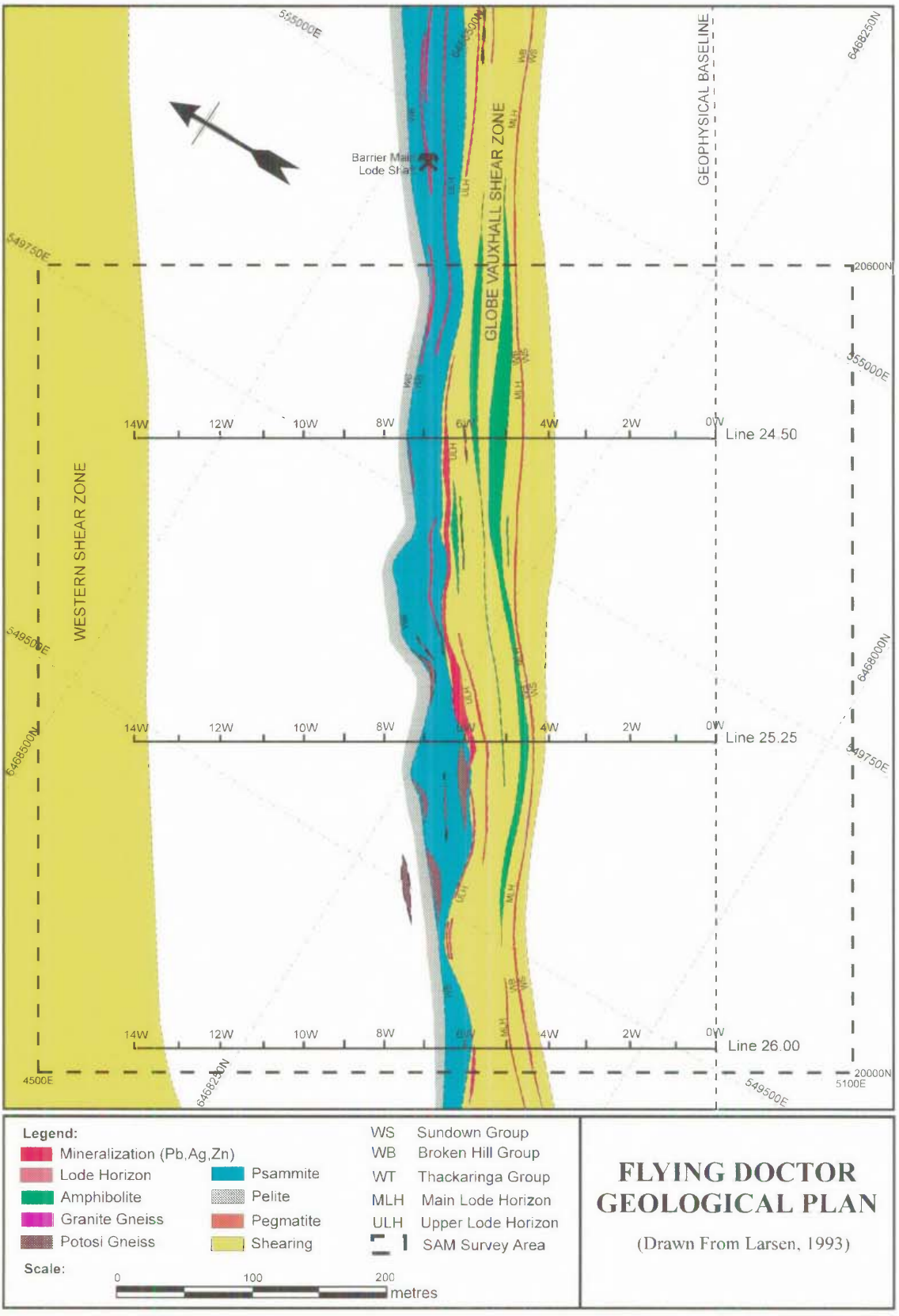

Figure 6-14. Flying Doctor Geological Plan (Drawn From Larsen, 1993).

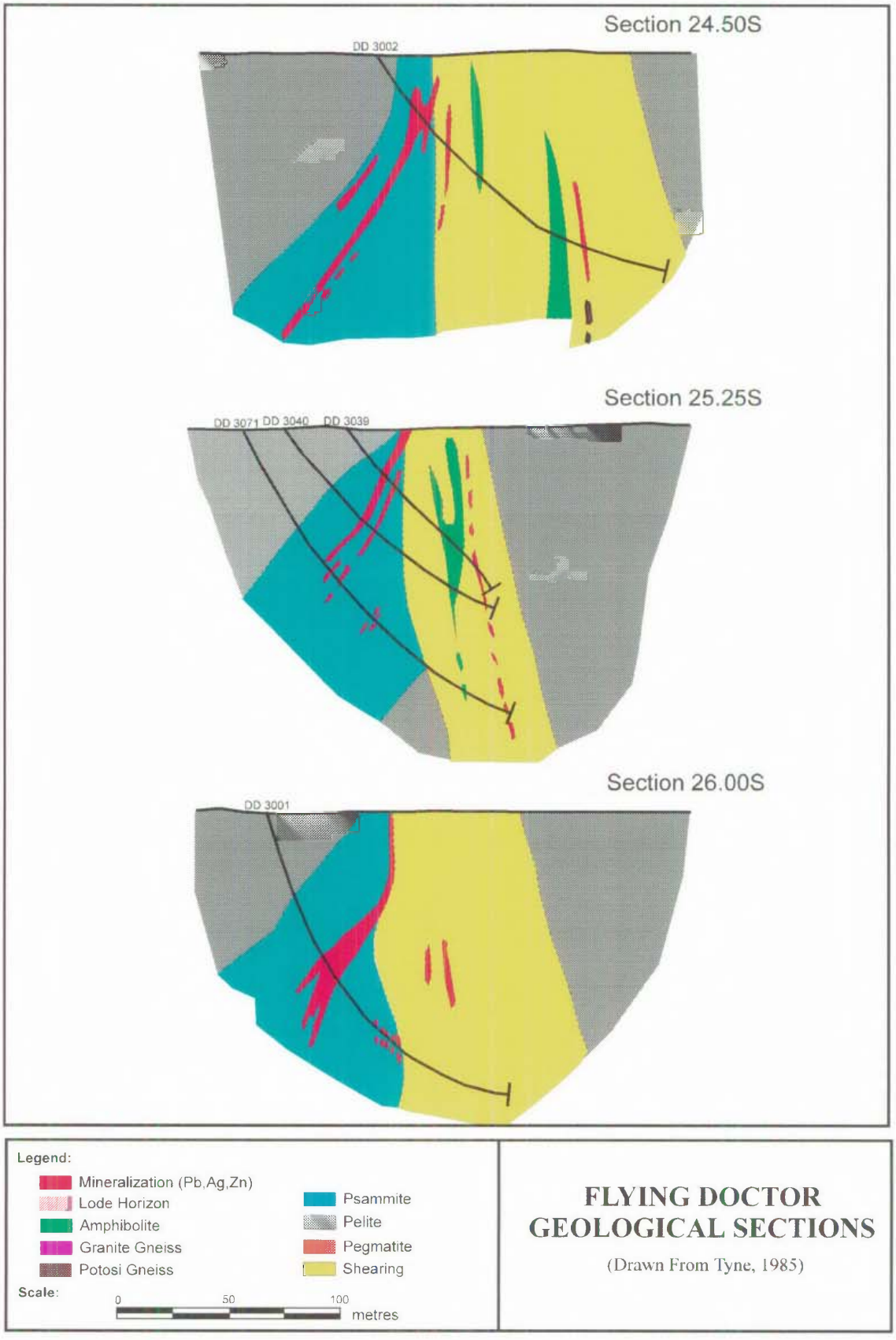

Figure 6-15. Flying Doctor Geological Sections (Drawn From Tyne, 1985).

"The major sulphide intersections occur near the boundary between a quartzitic gneiss and the retrograde shear zone and are equivalent to the ULH. ... Although the sulphide body is generally tabular and dips steeply to the west, it shows a considerable variation in cross-sectional shape over the 450m strike length between Lines 24.50 and 26.00. The narrow sulphide intersections within the shear zone are equivalents of the MLH. This mineralisation appears to have been remobilised during the development of the Globe Vauxhall retrograde shear, and as a result is conformable with the shear zone boundaries" (Tyne, 1987, 287).

The host rocks are sillimanite and quartzitic gneiss. Some surface traces of lode horizon rocks can be observed at about 6 W on the grid lines. However, there is no gossanous outcrop to indicate the presence of buried sulphide concentrations. The Globe Vauxhall Shear Zone parallels the surface projection of the ULH and the MLH.

6.3.2.1 Form of the Mineralisation

The character of the mineralisation at the Flying Doctor site has been summarised by Widdop *et al.* (*ibid.*, 14) as follows

"The Pb-Ag-Zn mineralisation consists predominantly of coarse metamorphic intergrowths of galena and sphalerite (marmatite) together with microscopic inclusions of native silver and silver bearing minerals. Although the intersections of higher grade sulphides generally consist of medium to coarse grained stratiform and locally remobilised sulphides, fine-grained disseminated stratiform sulphides are also common and occur together with coarse sulphides... Sulphides are most commonly hosted by the lode types but occur in a wide range of rock types. Both stratiform and remobilised stratabound sulphides occur within the lode horizon rock types ... The sulphide mineralisation consists predominantly of: galena + sphalerite (var. marmatite) -- minor pyrrhotite, chalcopyrite and pyrite ± accessory arsenopyrite, loellingite and rare accessories .. Common gangue mineralogies in intersections are, in general order of abundance; quartz, gahnite, f.g. muscovite, biotite, chlorite, K-feldspar, sericite altered sillimanite".

Widdop *et al.* (*ibid.*, 14) describe extensive development of the Globe Vauxhall and Western retrograde schist or shear zones within the area as representing:

"ductile shear deformation within which the original mineralogies of the prograde metamorphic gneisses appear to have been altered, overprinted and recrystallised resulting in the formation of retrograde schists consisting of quartz + sericite ± chlorite ± biotite ± accessory staurolite, chlorotoid".

6.3.3 Prior Geophysics

An evaluation of geophysical techniques with respect to their applicability to exploring for deposits similar to Flying Doctor has been compiled by Bishop (1989). Of the techniques discussed, electromagnetic (EM) techniques were considered the most successful followed by induced polarisation. Magnetics and radiometrics failed to detect the deposit. The techniques relevant for comparison with SAM are IP and magnetic induced polarisation (MIP).

6.3.3.1 Induced Polarisation (IP) / Resistivity

A gradient array Induced Polarisation / Resistivity survey is described by Tyne (1985). The results of the survey are shown in Figure 6-16. The survey was conducted with a current dipole spacing of 3600 ft (1100 m). And a potential dipole spacing of 100 ft (30.5 m). The distance between survey lines was 250 ft (76 m). The results indicate a region of low resistivity and IP response in the south-western corner of the grid. According to Tyne (*ibid.*), this appears to be related to a conductive layer of soil cover in the area. The data generally reflect the thickness of soil cover over the survey area. There is no localised resistivity or IP anomaly which could be attributed to the mineralisation. Tyne (*ibid.*) suggests that the large potential dipole spacing may have resulted in serious loss of resolution of the anomaly.

Dipole-dipole IP surveys also described by Tyne (*ibid.*) were more successful in defining the mineralisation. Representative pseudosections from Line 25.25S are depicted in Figure 6-17. The resistivity pseudosection shows a strong conductor at about 600 W flanked by a resistive unit on the east and a thin conductive surface layer overlying resistive host rock on the west. The chargeability and phase pseudosections both show distinct anomalies over 600 W. Another significant anomaly situated at about 1400 W is attributed to pyrite mineralisation within the Western Shear Zone. Of interest is that the western IP anomaly is not associated with an appreciable resistivity low.

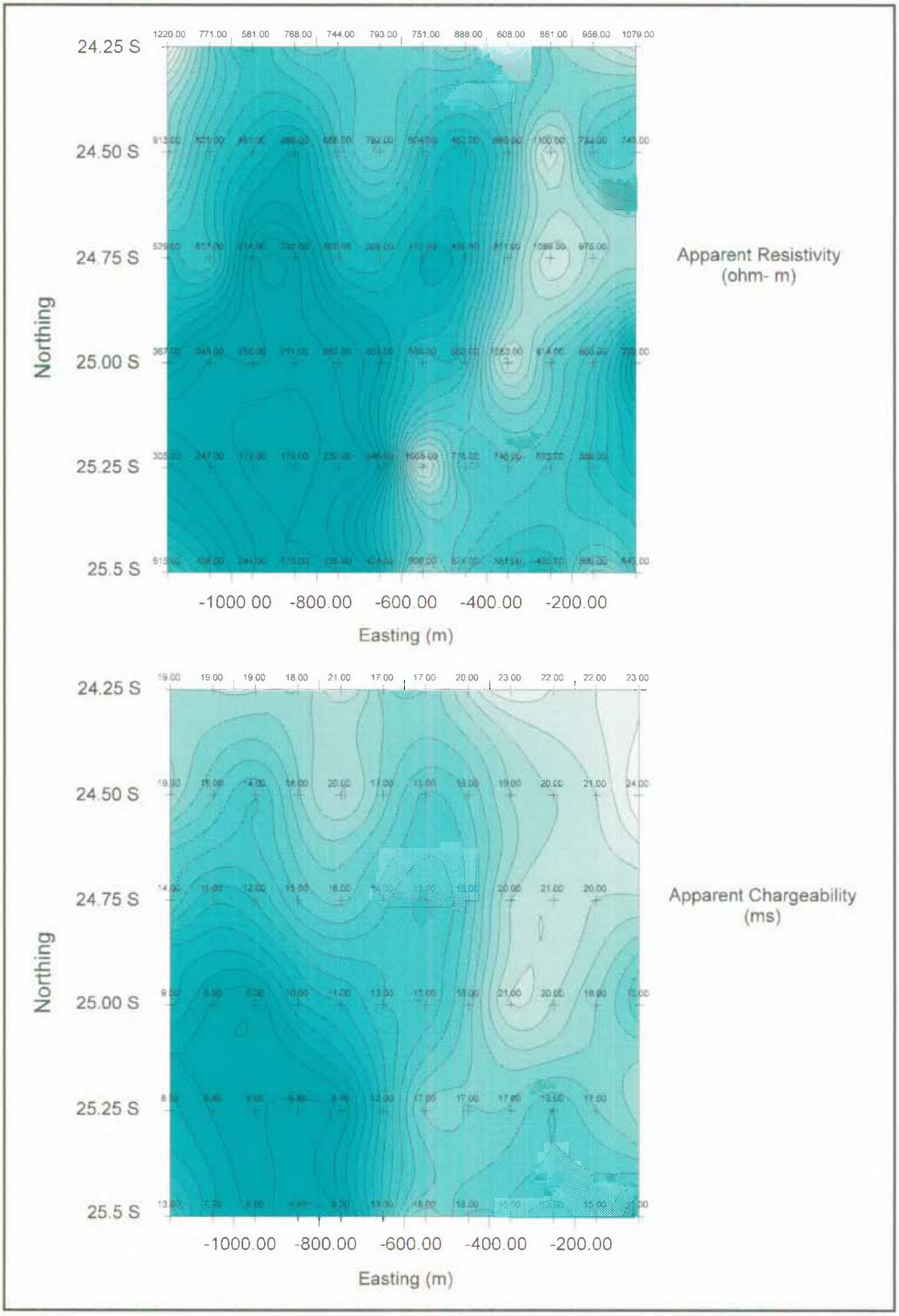

Figure 6-16. Gradient Array Resistivity and Induced Polarisation Survey. Flying Doctor Prospect (After Tyne, 1987).

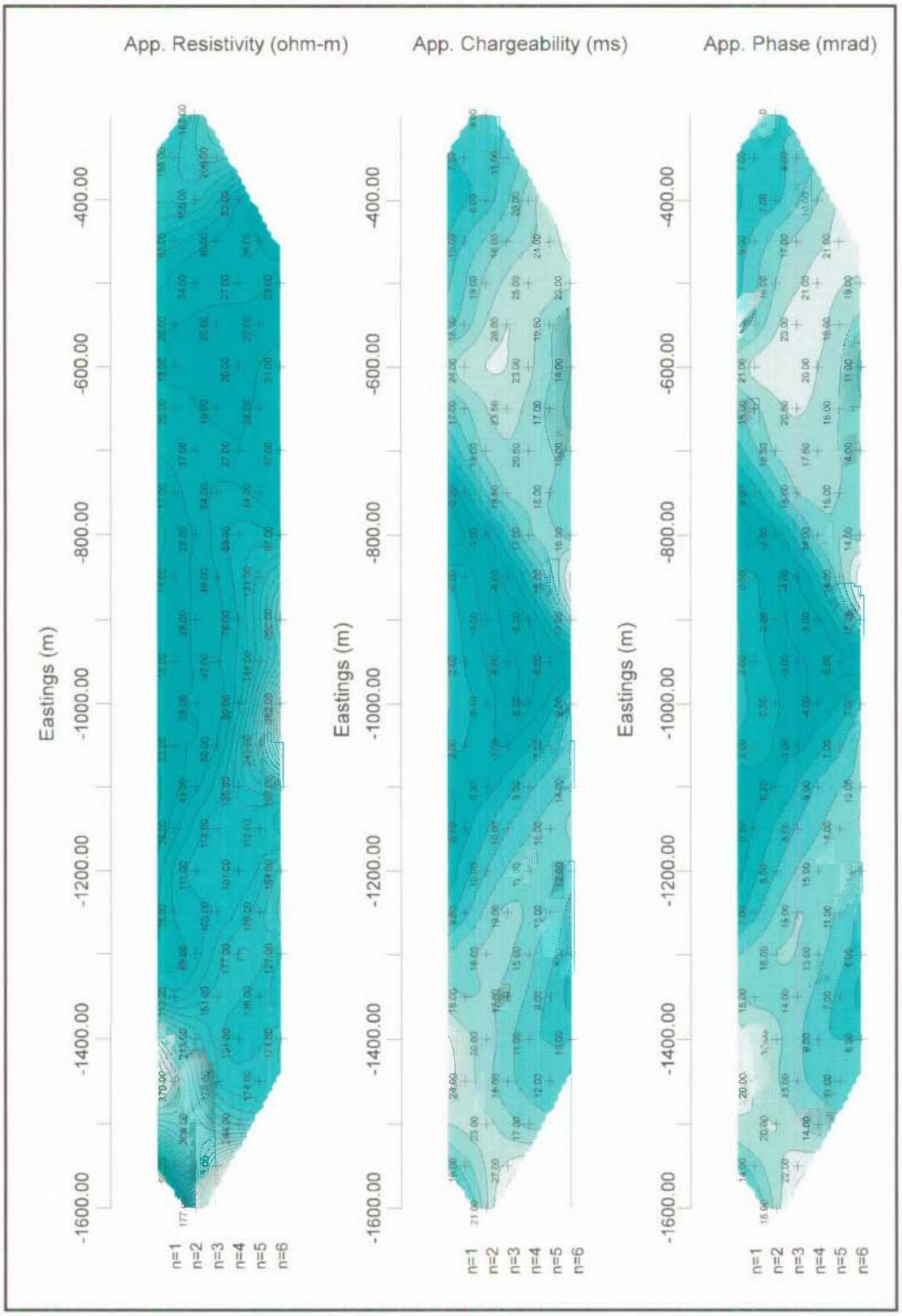

Figure 6-17. Dipole-dipole resistivity and IP profile - Line 25.25 S. Flying Doctor Prospect (After Tyne, 1987).

6.3.3.2 Magnetic Induced Polarisation (MIP)

As described in Chapter 2, the MIP method uses a single component magnetometer to measure IP and resistivity effects as opposed to SAM which uses a total field magnetometer. The techniques are otherwise very similar in field practice. Test MIP surveys were conducted by Scintrex over Lines 25.25 S, 25.75 S and 26 S (Howland-Rose, 1978). Both frequency domain and time domain measurements were made during the survey. Time domain profiles recorded on Line 25.25 S are shown in Figure 6-18. The survey resulted in a strong IP response over the mineralisation. The normalised magnetic field response (H_N) indicated a broad conductive zone with peaks occurring at 700 W and 800 W. However, the response was less defined over the other survey lines. The frequency domain parameters provided similar results as shown in Figure 6-19. The parameters Relative Phase Shift (RPS) and percent frequency effect (PFE) are also measures of the IP response and correlate well with the time domain parameter. The MIP technique showed promise in detecting the mineralisation. However, as pointed out by Bishop (*ibid.*), the lack of coverage with MIP meant that the superiority of the technique over EIP was not established at Flying Doctor.

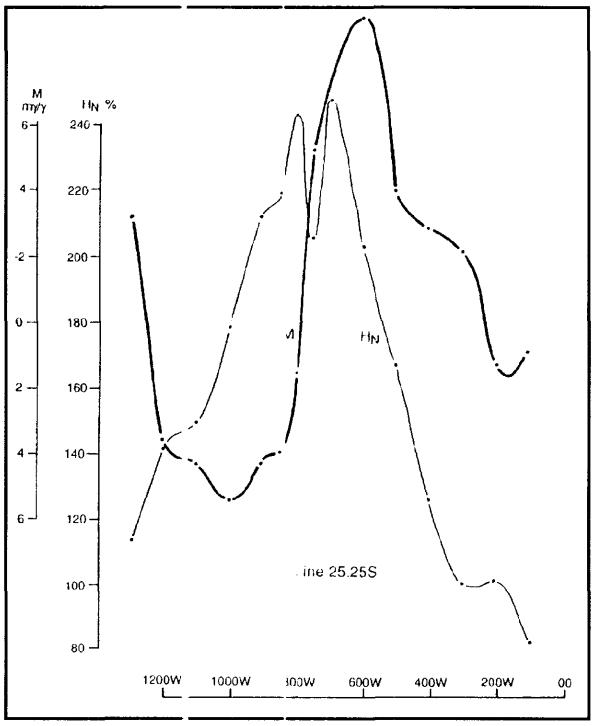

Figure 6-18. Time domain MIP response - Line 25.25 S (After Bishop, 1989).

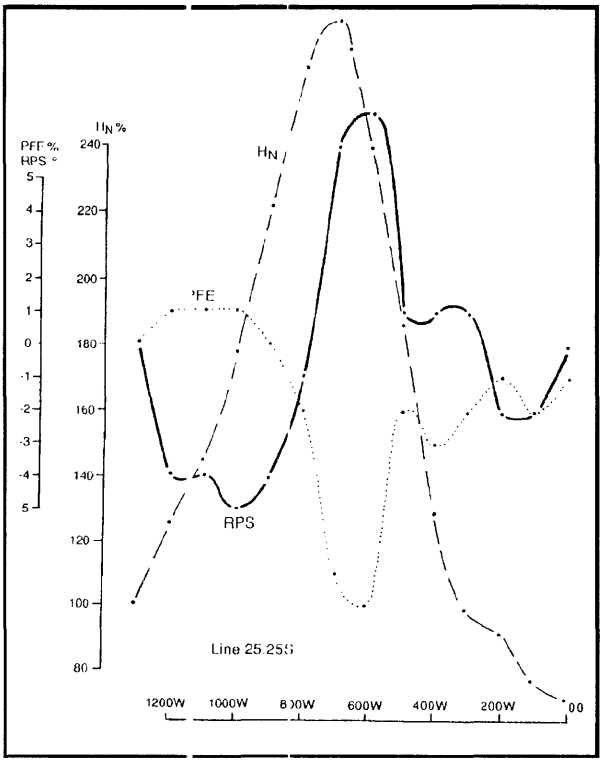

Figure 6-19. Frequency domain MIP response - Line 25.25 S (After Bishop, 1989).

6.3.4 SAM Field Procedure

In recent years, a metric coordinate system had been established at the Flying Doctor site (see Figure 6-14). The SAM survey described in this paper was conducted with reference to the metric grid. Grid North was orientated at 50° magnetic. The magnetic inclination, *I*, was approximately -64.3°.

The two current electrodes C1 and C2 were embedded at 4800 mE, 19800 mN and 4800 mE, 20800 mN respectively. The survey area was located within the boundaries 4500 mE to 5100 mE and 20000 mN to 20600 mN (600 m x 600 m). However, a small section could not be surveyed due to the existence of buildings in the area. The wire feeding the electrodes was laid out in a U-shape to the west of the centre line (4800 mE). Coordinates defining the location of the wire are as follows: 4800 mE, 19800 mN (C1); 4200 mE, 19800 mN; 4200 mE, 20800 mN; 4800 mE, 20800 mN (C2). The layout of the survey is shown in Figure 6-8. Traverses were surveyed on foot in an east-west (local) direction. The line interval was 10 m.

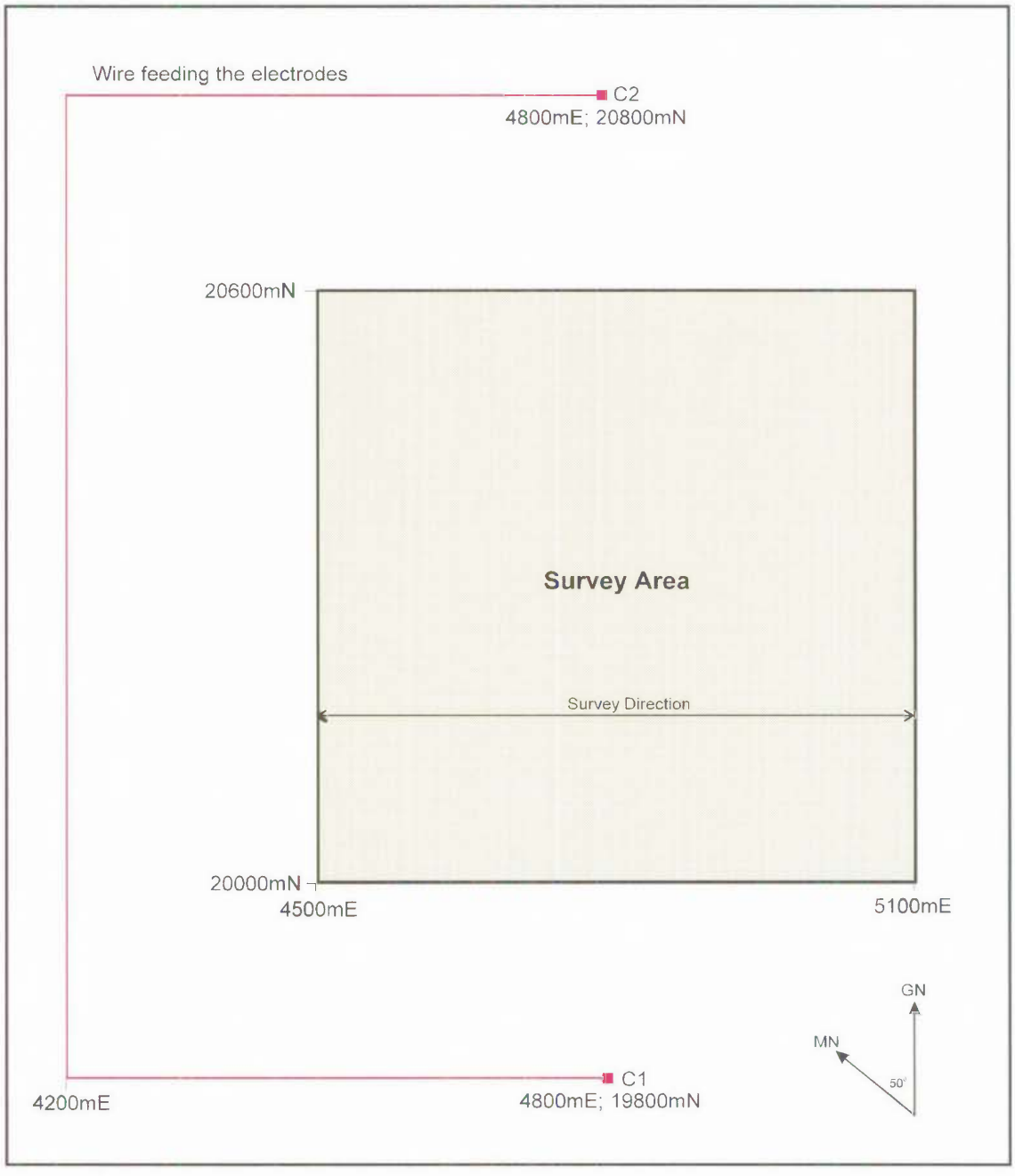

Figure 6-20. Layout of the Survey Area showing the location of the electrodes and current-bearing wire.

6.3.5 Results

6.3.5.1 Total Magnetic Intensity (TMI)

The spatially-varying magnetic field was extracted from the combined data set by lowpass filtering and then sampled at 0.5 m intervals. After correcting for diurnal variation, the data were gridded and imaged. The image is shown in Figure 6-21. In all the following images, the colour assignment ranges from purple for low amplitudes to red for high amplitudes.

As can be seen from the figure, there is a magnetic gradient increasing to the north-east corner of the survey area. As was mentioned previously, the deposit has been extensively drilled and the discrete dipolar anomalies aligned along the axis of the mineralisation are due to steel drillhole collars. The linear features to the south and east of the image are due to fences. There are subtle linear features aligned south-west to north-east which cross the mineralisation. However, there appears to be no distinct magnetic signature from the mineralisation itself.

6.3.5.2 Total Field Magnetometric Resistivity (TFMMR)

The corrected TFMMR data is shown in Figure 6-22. As can be seen in the figure, there is a significant linear "high" coincident with the Globe Vauxhall Shear Zone. In addition, there are a number of well-defined linear features some of which parallel the strike of the mineralisation and some which cut obliquely across strike.

Reduction to the pole resulted in the image shown in Figure 6-23. Theoretically, this should have the effect of aligning the TFMMR "highs" over conductors. The result is shown in Figure 6-23.

In an attempt to enhance the more subtle linear features in the data set, the first vertical derivative of the data from Figure 6-23 was calculated. The result of this processing is an extraordinary amount of structural detail as shown in Figure 6-24.

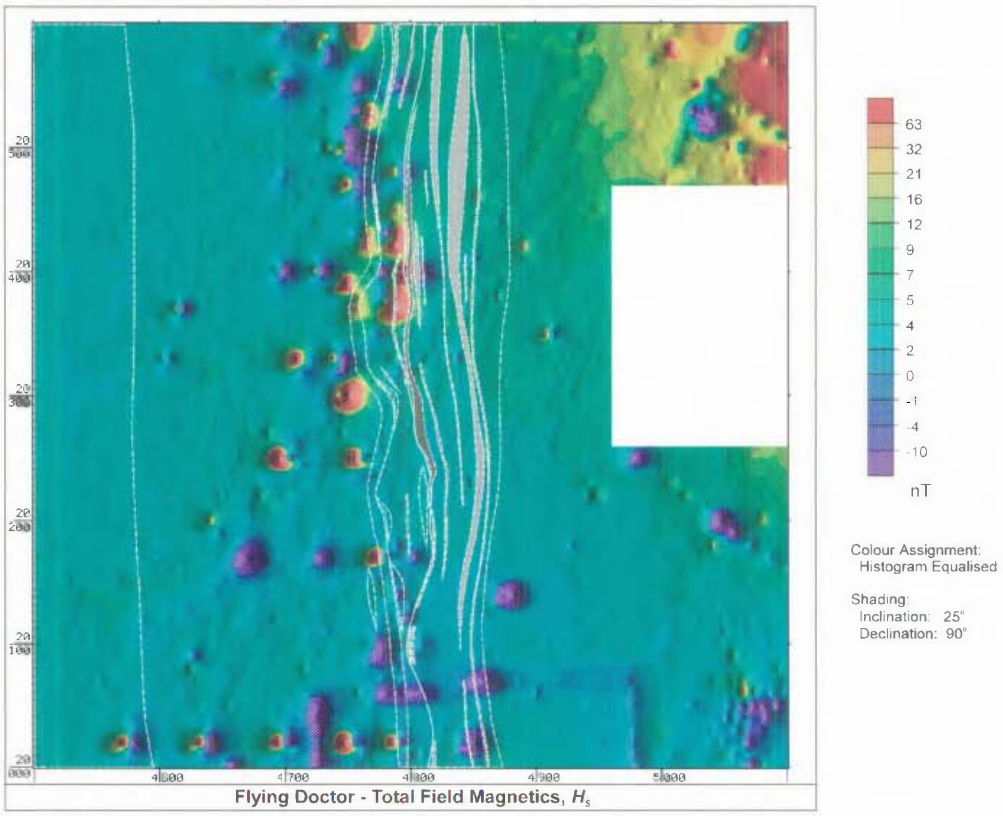

Figure 6-21. Flying Doctor - Total Magnetic Intensity, H_S with geological overlay.

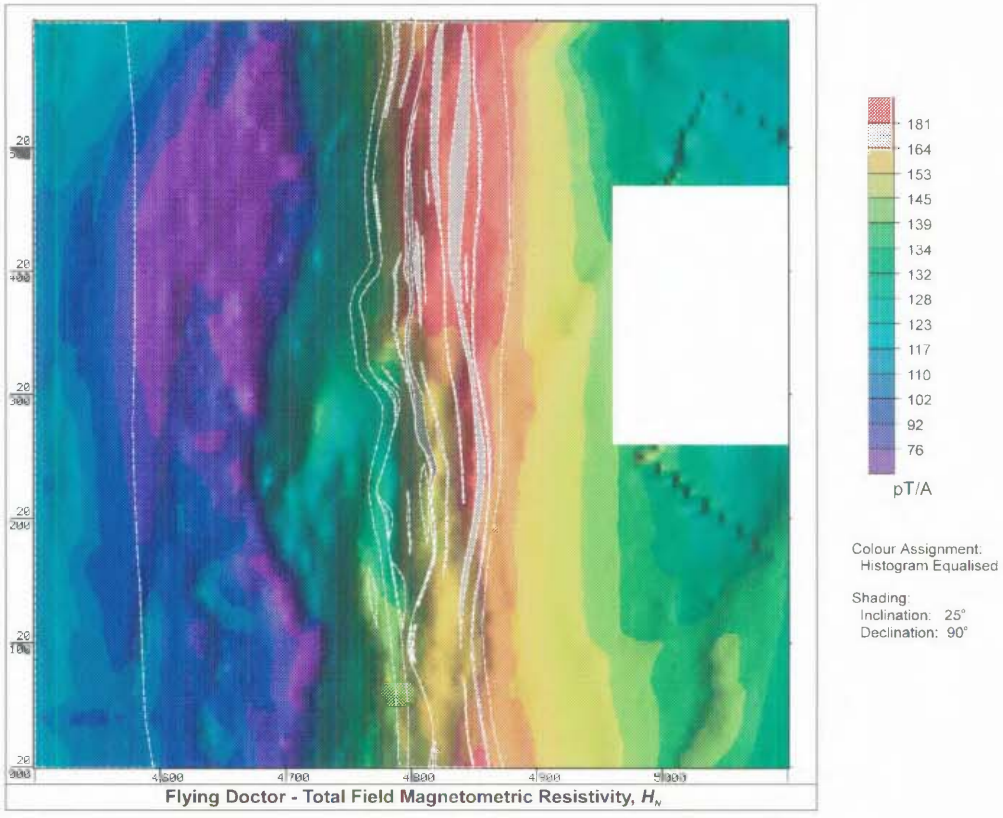

Figure 6-22. Flying Doctor - Normalised TFMMR, H_N.

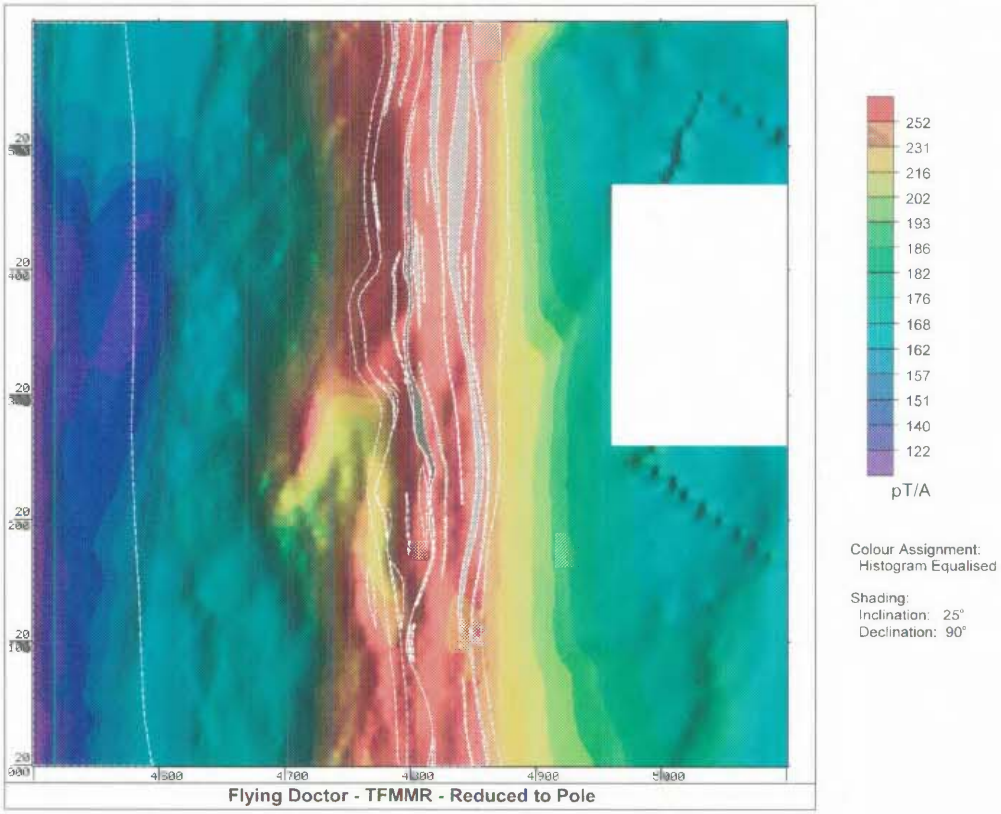

Figure 6-23. Flying Doctor TFMMR, H_N - Reduced to Pole.

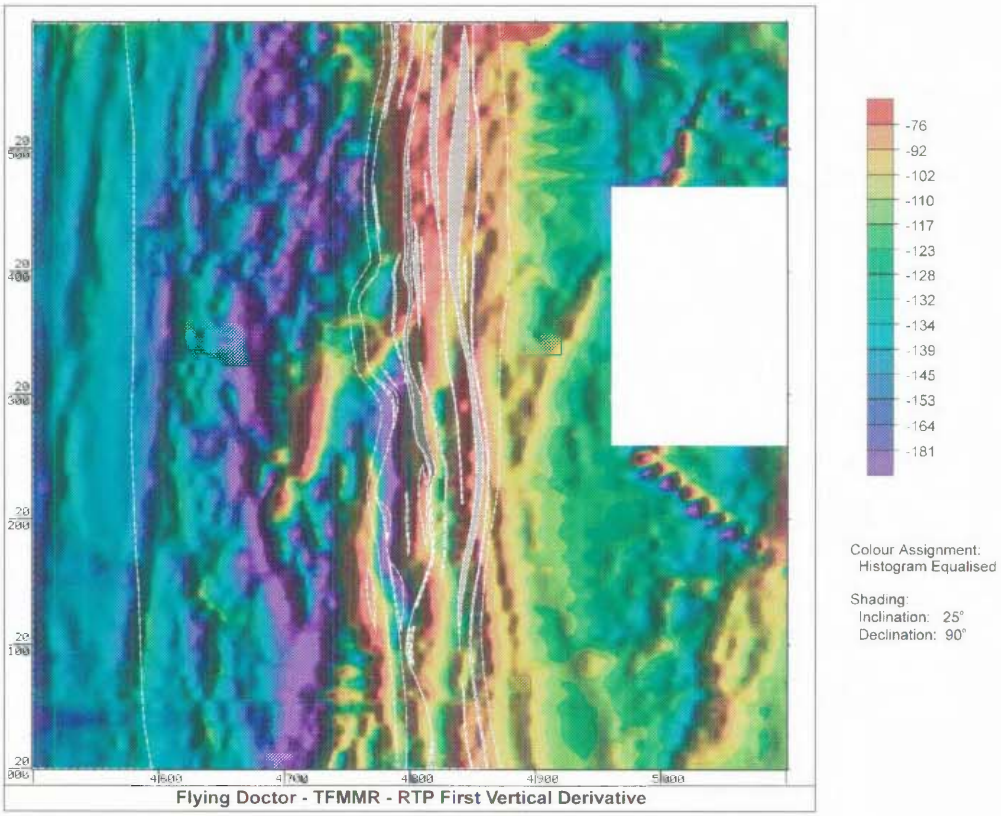

Figure 6-24. Flying Doctor First Vertical Derivative of TFMMR, H_N - RTP.

6.4 Evaluation of the Feasibility Trials

The basic field procedure used for the feasibility studies was found to require little modification from that which had been developed for conducting High Definition Magnetic (HDM) surveys over the last fifteen years. It was anticipated that survey production rates similar to those achieved for HDM surveys should be routinely possible. Sub-metre sample intervals in both TFM and TFMMR were found to be feasible at walking speed, although initial indications from the trials suggest that sample intervals of 2-3 m should be adequate to sample the electromagnetic field resulting from the induced galvanic current flow.

The data acquisition procedures that were adopted for the feasibility trials imposed inefficiencies that were unique to the experimentation being performed. The desire to record the full magnetic waveform at 200 samples per second for research purposes resulted in:

(i). A reduction of survey production by a factor of about 50% due to the time taken to upload data when memory was filled, and

(ii). Data storage and processing problems due to the volume of data recorded.

Several feasibility studies were conducted over various types of geological targets using the TFMMR/TFMMIP configuration. In each case, the results showed good correlation with the known geology and confirmed that the SAM technique performs in practice as was predicted from theory. The signal-to-noise ratios in the recorded parameters were high and sub-metre measurement intervals were found to be achievable at continuous walking speeds of traverse.

The higher spatial resolution (up to 100 times greater than conventional electrical methods) proved capable of providing significantly more diagnostic information than has been previously possible using conventional electrical and electromagnetic methods. It was also found to provide detailed electrical mapping with definition equivalent to that obtained in High Definition Magnetic mapping.